Orogenic quiescence in Earth's middle age

Ming Tang[1*], Xu Chu[2], Jihua Hao[3], Bing Shen[1]

[1]Key Laboratory of Orogenic Belt and Crustal Evolution, MOE; School of Earth and Space Science, Peking University, Beijing 100871, China.
[2]Department of Earth Sciences, University of Toronto, 22 Ursula Franklin Street, Toronto, Ontario M5S 3B1, Canada.
[3]Department of Marine and Coastal Sciences, Rutgers University, 71 Dudley RD, New Brunswick, New Jersey 08901, USA.
[*]Corresponding author. Email: mingtang@pku.edu.cn

Abstract

Mountain belts modulate denudation flux and hydrologic processes and are thus fundamental to nutrient cycling on Earth's surface. We used europium anomalies in detrital zircons to reconstruct the evolution of crustal thickness over Earth's history. We show that the average thickness of active continental crust varied on billion-year timescales with the thickest crust formed in the Archean and Phanerozoic. By contrast, the Proterozoic witnessed continuously decreasing crustal thickness, leaving the continents devoid of high mountains until the end of the eon. We link this gradually diminished orogenesis to the long-lived Nuna-Rodinia supercontinent, which altered the mantle thermal structure and weakened the continental lithosphere. This prolonged orogenic quiescence may have resulted in a persistent famine in the oceans and stalled life's evolution in Earth's middle age.

One sentence summary

The long-lived Nuna-Rodinia supercontinent diminished mountain building processes in Earth's middle age.

Earth's continents have a highly skewed elevation distribution. The vast majority of the continental areas lies close to sea level due to the balance between erosion and deposition (*1*). However, at convergent plate boundaries, active mountain-building processes, known as orogenesis, generate substantial uplift. These mountainous terrains, though minor by area, profoundly influence global denudation and hydrologic processes on land (*2-5*).

Mountain belts owe their high elevations to crustal thickening, which, in turn, is driven by tectonic compression and magmatic inflation (*6*). Meanwhile, uplift increases erosion efficiency and induces gravitational spreading (*7*), which counters crustal thickening. After magmatism and tectonic compression terminate, erosion and collapse of the orogen prevail, and the crust quickly loses its thickness and elevation as it ages. Thereby, mountains are ephemeral and the history of mountain building has been constantly erased and overprinted. The remnant, with respect to thickness, is not representative of the crust when it formed. This preservation issue poses great challenges to track orogenesis in deep time.

Here we reconstruct mountain building history using a recently calibrated zircon-based crustal thickness proxy (*8*). Detrital zircons are derived from a variety of crustal rocks and naturally sample large tracts of the continental crust exposed to erosion. Owing to their refractory nature, zircons survive most erosion and weathering processes, remain chemically intact, and thus provide a continuous record of magmatic history where fragmented rock records fail (*9*). The zircon-based crustal thickness proxy utilizes the pressure-sensitive Eu systematics during magmatic differentiation, which is recorded as Eu anomalies (Eu/Eu*, chondrite normalized $Eu/\sqrt{Sm \times Gd}$) in crystallizing zircons. We filtered out metamorphic zircons and zircons derived from S-type granites based on zircon Th/U ratios and P contents, respectively (*10*).

Our approach calculates the thickness of all magmatically active crust. We term this crust the active continental crust. The majority of active continental crust forms at convergent plate margins due to oceanic plate subduction and continent-continent collision. The overriding continental plate, in which orogenic magmatisms develop, could be either reworked pre-existing crust or juvenile crust. In both cases the resulting mountain belts interact with the surface environment in essentially the same way. Thus, we did not filter our compilation with zircon Hf or O isotope data. The scope of this study and our approach thereby differ from a previous study by Dhuime and coworkers (*11*) who utilized Sr isotopes and Nd model ages to specifically constrain the thickness of juvenile crust.

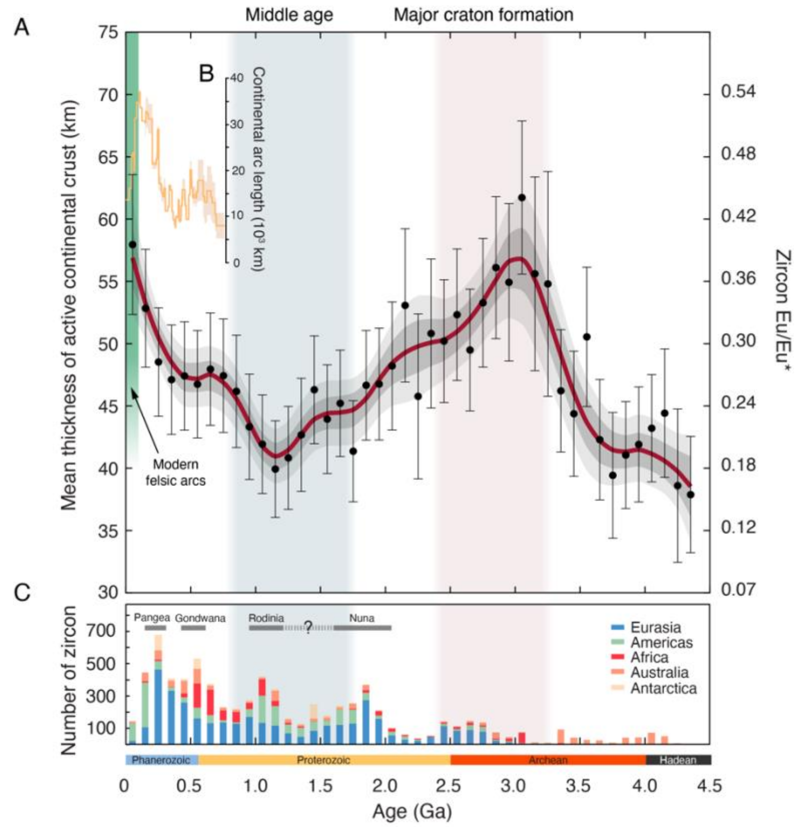

Figure 1. Reconstructed thickness of active continental crust over Earth's history. (**A**) This reconstruction is based on over 14,000 analyses of detrital zircons from around the globe (*10*). Data are plotted as binned averages (bin size = 100 Ma) with two standard errors (2 SEM). A smoothed trend bracketed by 68% and 95% confidence intervals is shown by the red curve with shaded envelopes. We take zircon crystallization ages as the ages of synmagmatic orogenesis. The time window of major craton formation (pink band) is from ref (*12*). (**B**) The length of continental arcs in the last 750 Ma (means enveloped by uncertainty intervals) is from ref (*13*). (**C**) Number of detrital zircons from each continent within each 100 Ma bin.

The reconstructed thickness of active continental crust averages 50-60 km in the Phanerozoic, and shows a thickening trend toward the present (Fig. 1A). The thick active continental crust in the Phanerozoic is consistent with the observations that most of the modern felsic arcs are built on crust > 40 km (*14*). We also find that the pattern of reconstructed crustal thickness mimics the trend of continental arc length in the last 750 Ma (Fig. 1B). Because continental arcs represent the thick endmember of active crust, this pattern similarity affirms that the crustal thickness reconstructed from detrital zircons faithfully tracks the overall mountain building activity in the past.

The Precambrian active continental crust varies substantially in thickness over time (Fig. 1). The active crust became progressively thicker from the Hadean to the Archean and reached a maximum average thickness of 55-65 km in the Meso- to Neoarchean (3.2–2.5 Ga). The emergence of thick felsic crust in the Meso- to Neoarchean coincides with the peak of craton formation (*12*), which may also result from compressive tectonics (*15, 16*). The lack of thick active crust and thus orogenesis in the Paleoarchean and Hadean (Fig. 1) suggests that lateral plate convergence may have been weak in the first billion years of Earth's history. We note that this speculation is based on a limited number of detrital zircons from this time period, and may be tested when additional detrital zircon data become available.

In the Proterozoic, the thickness of active continental crust exhibits a "V" shaped temporal pattern. Crustal thickness declined continuously from the Paleoproterozoic through the end of the Mesoproterozoic. At 1.3–1.0 Ga, the average thickness of active crust may have been as low as 40 km, close to the crustal thickness of the heavily eroded continental interior. This would imply that, on 100 Ma timescales, the continents at that time were far less mountainous than today.

This long-term quiescence in mountain building coincides with a substantial reduction of subduction flux in the Proterozoic (*17*) inferred from Nb/Th of the depleted mantle (*18*) and ^{4}He/^{3}He of ocean island basalts (*19*). Reduced orogenesis and subduction flux may be linked to the unique supercontinent cycles in the Proterozoic. Supercontinents insulate the underlying mantle, and this "blanketing" effect can profoundly alter mantle thermal structure (*20-22*). As a consequence, the mantle beneath a supercontinent becomes hotter, whereas the mantle beneath an oceanic domain cools down (*22*) for a thermal balance. Cooling increases sub-oceanic mantle viscosity and thus decreases oceanic plate velocity.

The Proterozoic witnessed two supercontinents: Nuna (Columbia) and Rodinia. Nuna was assembled between 2.1–1.8 Ga (*23*), then it broke up between 1.6–1.2 Ga, followed by the amalgamation of Rodinia at 1.2–0.9 Ga (*23*). However, a growing body of evidence suggests that the breakup of Nuna was limited, and it transitioned to Rodinia with only minor reconfiguration (*24, 25*). This unconventional transition is also supported by the paucity of passive margins in the Mesoproterozoic (*26*). In this regard, Nuna and Rodinia may be viewed as one largely coherent supercontinent cycle (Nudinia, (*27*)), spanning from the late Paleoproterozoic to the early Neoproterozoic (*28*). The mantle thermal structure, altered by the long-lived supercontinent lid, may have led to substantial cooling of the sub-oceanic mantle to the point that plate tectonics operated intermittently until the breakup of Rodinia.

Prolonged heating of the continental lithosphere may prompt widespread low-pressure–ultrahigh-temperature metamorphism and intraplate anhydrous magmatism within the continents (*20*), which are distinctive in the mid-Proterozoic metamorphic (*29*) and igneous (*30*) records. The Grenville orogen formed between 1250–980 Ma has long been regarded as a prototype of the Himalaya-Tibet orogen (*31*). However, the massive anorthosite massifs, dike swarms, peralkaline shoshonite and ubiquitous A-type granite suites that characterizes the Grenville orogen (and the Sveconorwegian orogen) have been rare in Phanerozoic orogens (*28, 32*). Intense heating could thermally weaken the lithosphere, causing thickened crust to relax rapidly. Detrital zircons of broadly-defined Grenvillian ages (1250–980 Ma) from North America further show that the Grenville orogen differs from its Phanerozoic counterparts. In southern

Tibet and the North American Cordillera, most detrital zircons record 50–70 km crustal thicknesses, whereas in the Grenville, crustal thickness peaks at 40 km (Fig. 2).

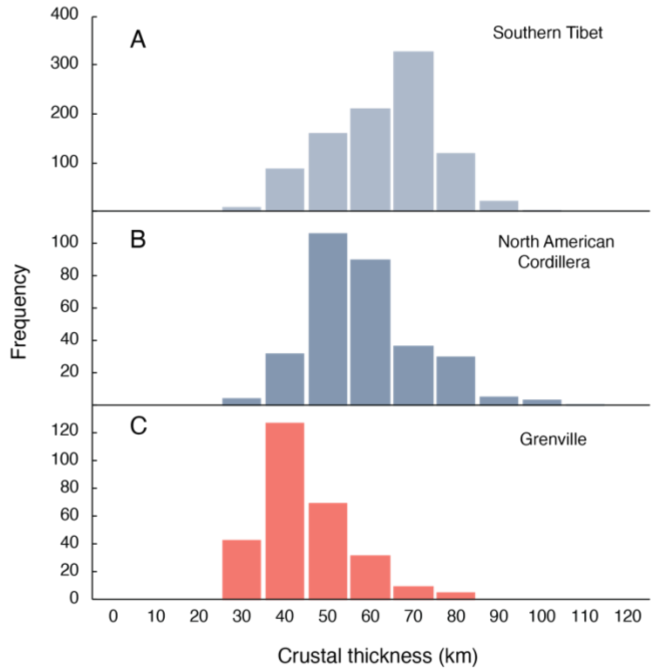

Figure 2. Reconstructed crustal thicknesses for southern Tibet, North American Cordillera and North American Grenville. We assumed that North American detrital zircon populations at 230–50 Ma and 1250–980 Ma are primarily sourced from the North American Cordillera and Grenville orogens, respectively. Southern Tibet detrital zircon data (100 Ma to present) are from ref (*8*).

Long-term quiescence in mountain building may have a profound influence on the hypsography of Earth's surface. The elevation of continent freeboard is determined by a number of factors including the thickness of the continental crust and oceanic crust, densities of the crust and mantle and seafloor depth (*33, 34*). For simplicity, we extrapolate the conditions of isostasy on modern Earth to the past. We find that, if sea level was not dramatically different, most of the active continental crust in the mid-Proterozoic may have had elevations of no more than 1–2 km, in contrast to 3–5 km in the succeeding Phanerozoic era (Fig. 3A).

The loss of elevation contrasts between the active continental crust and oceans would substantially reduce erosion rate (*2*) and the intensity of the hydrologic cycle (*35*) on the continents, leading to a subdued weathering flux in this time period. This effect is shown by the similar active continent elevation and seawater Sr isotope curves in the Proterozoic (Fig. 3A, B). With muted continental weathering, nutrient supply to the oceans declines. The scarcity of phosphorus, molybdenum, and other trace metals would dampen primary productivity and reduce O_2 production (*36*), which would, in turn, further decrease the molybdenum flux from the continents (*37*) and enhance molybdenum and phosphorus removal from the Proterozoic oceans (*37-39*).

Eventually, a widespread famine and a collapse of primary productivity may occur in the Proterozoic oceans. This is reflected by the extremely low molybdenum in black shales, disappearance of sedimentary phosphorite, and strongly negative $\Delta^{17}O$ evaporates and carbonate-associated sulfate between 1.8–0.8 Ga (*37, 40-42*) (Fig. 3D-F). The systematic decline in the atmospheric O_2 into the mid-Proterozoic is corroborated by the decreasing uranium concentrations in black shales (*43*) (Fig. 3C) and the fall of seawater sulfate level (*44, 45*) after the initial rise of atmospheric O_2 between 2.5–2.0 Ga, the Great Oxidation Event. Biological evolution may have been largely stalled during this one-billion-year orogenic quiescence, a time period often referred to as the "boring billion" (*46, 47*).

The middle age orogenic quiescence came to an end in the Neoproterozoic (Fig. 1A), a time corresponding to the termination of the long-lived Nuna-Rodinia supercontinent. The breakup of the Nuna-Rodinia supercontinent may have relaxed the thermal contrast between the sub-oceanic and sub-continental mantle and established modern-style plate tectonics. As mountains reappeared on the continents, nutrient supply to the oceans was enhanced, which catalyzed surges in biological productivity and resumed surface oxidation. Efficient orogenesis appears to be maintained ever since (Fig. 1). The sustained high erosion and weathering rates promoted organic carbon burial as evidenced by a systematic ^{13}C enrichment in Phanerozoic carbonates (*48*). With the emergence of a fully oxidized atmosphere-ocean system, the planet was eventually primed for the arrival of metazoans in the Cambrian (*49*).

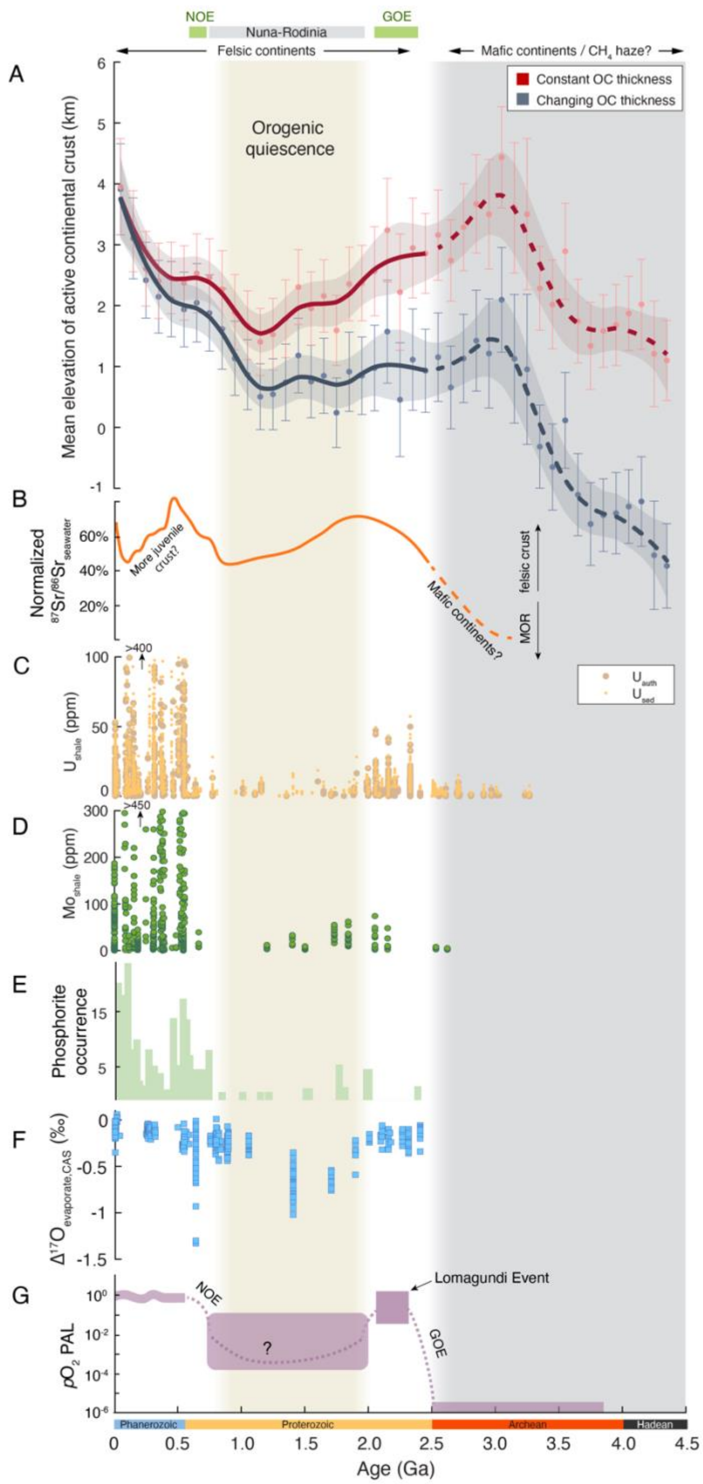

Figure 3. Elevation of the active continental crust over Earth's history and evolution of Earth's surface environment. (**A**) Elevation plotted as binned averages (bin size = 100 Ma) with two standard errors (2 SEM). Also shown are the smoothed trends bracketed by 95% confidence intervals. The elevation of active continental crust can be calculated from on our reconstructed crustal thickness using an isostasy model (*10*). We consider two endmember scenarios of oceanic

crust thickness, one with constant thickness over time and the other decreasing thickness from the Hadean to present-day (*10*). (**B**) The normalized seawater Sr isotope curve is from ref (*50*), which removes the radiogenic decay effect and thus reflects the contributions from mid ocean ridge (MOR) and the felsic continental crust. The Sr isotope curve decouples from that of the elevation since ~450 Ma, which is probably due to an increasing contribution from juvenile crust with MOR-like Sr isotopes (*51*). (**C**) Uranium and authigenic uranium concentrations in black shales (*43*). (**D**) Molybdenum concentrations in black shales (*37*). (**E**) Sedimentary phosphorite occurrence (*40*). (**F**) $\Delta^{17}O$ in evaporate and carbonate associated sulfate (*42*). (**G**) Atmospheric oxygenation history. The purple fields are from refs (*52, 53*). The dashed curve in the Proterozoic field is our proposed path (schematic). NOE: Neoproterozoic Oxidation Event; GOE: Great Oxidation Event.

Supplementary Materials

Methods and Materials

Detrital zircon data compilation

We used a recently calibrated Eu/Eu*-in-zircon proxy to calculate crustal thickness. In short, this proxy is based on the empirical relationship between zircon Eu/Eu* and whole rock La/Yb ratio in intermediate to felsic rocks, the latter of which has been shown to correlate with crustal thickness in magmatic arcs (*54*). This detrital zircon approach is intrinsically biased such that it only sees intermediate to felsic crust. This is because mafic rocks are generally zircon-undersaturated. However, mafic crust has not been a major component of the continental crust since at least the late Archean (*11, 55, 56*). In addition, crust formed in orogenic belts is generally highly differentiated and almost certainly zircon-bearing (*57*). Therefore, this bias would have limited influence on discussions of continental crust evolution and orogenesis through time.

Our compiled global detrital zircon database contains over 14,000 chronological and trace element analyses of detrital zircon grains whose ages span from 4.4 Ga to present (see Database S1). The detrital zircons were extracted from modern and ancient terrigenous sedimentary deposits in Eurasia, Africa, Antarctica, North and South Americas, Australia according to source literatures (n = 33). We screened the detrital zircon database before applying the Eu/Eu*-in-zircon proxy. First, we removed zircons likely sourced from S-type granitoids (P contents > 750 ppm (*58*)) because zircon Eu/Eu* does not correlate with whole rock La/Yb in S-type granitoids. Second, we removed zircon analyses with high La concentrations (> 1 ppm) as these analyses are potentially compromised by inclusions. Finally, we filtered out zircons affected by metamorphic overgrowth (Th/U < 0.1 (*59*)). For zircons younger than 1000 Ma, we took ^{206}Pb-^{238}U ages as their crystallization ages; for older detrital zircons, we used ^{206}Pb-^{207}Pb ages as their crystallization ages to minimize the potential effect of Pb loss on age determination.

We did not apply any sample weights in calculating the binned crustal thickness and average crustal thickness trend (Fig. 1) because detrital zircons naturally sample large areas of the exposed continental crust.

Elevation calculation

The elevation of the active continental crust (H) shown in Fig. 3 was estimated from the reconstructed crustal thickness (Fig. 1) and the Airey isostasy principle:

$$h_{cc}*\rho_{cc}*g = h_{sw}*\rho_{sw}*g + h_{oc}*\rho_{oc}*g + h_m*\rho_m*g \quad (1)$$

$$H = h_{cc} - h_{sw} - h_{oc} - h_m \quad (2)$$

Where ρ_{cc}, ρ_{sw}, ρ_{oc} and ρ_m are the densities of the active continental crust (2.8 g/cm^3), seawater (1.0 g/cm^3), oceanic crust (3.0 g/cm^3), and mantle (3.3 g/cm^3), respectively, h_{cc}, h_{sw}, h_{oc} and h_m are the thickness of the active continental crust (reconstructed), seafloor depth near the trench (~5 km), the thickness of the oceanic crust and the height of the mantle column between the bottom of the oceanic crust and that of the continental crust, respectively, and g is acceleration due to gravity. Seafloor depth depends on the volumes and areas of the continents and oceans and is poorly constrained for the past. For simplicity, we assume that seafloor depth was largely constant over Earth's history. The average thickness of modern oceanic crust is roughly 7 km, but it may have varied significantly in the past. For example, Herzburg et al. (*60*) suggested that the oceanic crust may have been 25-35 km thick in the Archean due to larger degrees of mantle melting. We thus consider two endmember scenarios: one with a constant oceanic crust thickness (7 km) through time and another one in which the oceanic crust thickness progressively increases from the present-day 7 km to 30 km at 3.0 Ga, as shown in Fig. 3a.

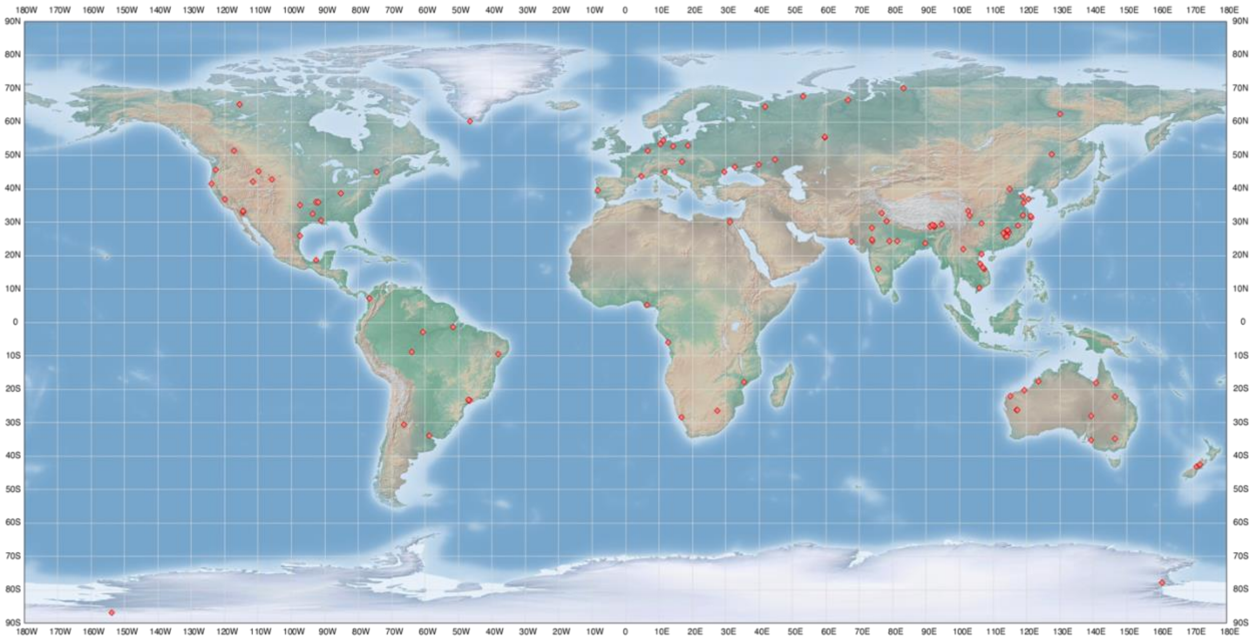

Fig. S1. Map showing sedimentary deposits (red dots) used to build the detrital zircon database in this study. See Database S1 for details.

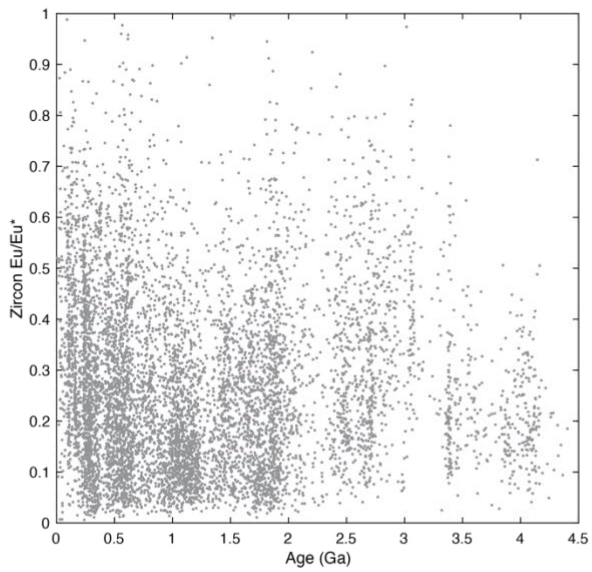

Fig. S2. Scatter plot of individual detrital zircon Eu/Eu* vs. crystallization age.

References

1. D. B. Rowley, Sea level: Earth's dominant elevation—Implications for duration and magnitudes of sea level variations. *The Journal of Geology* **121**, 445-454 (2013).
2. I. J. Larsen, D. R. Montgomery, H. M. Greenberg, The contribution of mountains to global denudation. *Geology* **42**, 527-530 (2014).
3. J. D. Milliman, K. L. Farnsworth, *River discharge to the coastal ocean: a global synthesis*. (Cambridge University Press, 2013).
4. L. R. Kump, S. L. Brantley, M. A. Arthur, Chemical Weathering, Atmospheric CO2, and Climate. *Annual Review of Earth and Planetary Sciences* **28**, 611-667 (2000).
5. A. J. West, A. Galy, M. Bickle, Tectonic and climatic controls on silicate weathering. *Earth and Planetary Science Letters* **235**, 211-228 (2005).
6. C.-T. A. Lee, S. Thurner, S. Paterson, W. Cao, The rise and fall of continental arcs: Interplays between magmatism, uplift, weathering, and climate. *Earth and Planetary Science Letters* **425**, 105-119 (2015).
7. C. T. A. Lee, in *Treatise on Geochemistry (Second Edition),* H. D. Holland, K. K. Turekian, Eds. (Elsevier, Oxford, 2014), pp. 423-456.
8. M. Tang, W.-Q. Ji, X. Chu, A. Wu, C. Chen, Reconstructing crustal thickness evolution from europium anomalies in detrital zircons. *Geology*, (2020).
9. C. J. Hawkesworth *et al.*, The generation and evolution of the continental crust. *Journal of the Geological Society* **167**, 229-248 (2010).
10. Materials and Methods are available as Supplementary Materials on Science Online
11. B. Dhuime, A. Wuestefeld, C. J. Hawkesworth, Emergence of modern continental crust about 3 billion years ago. *Nature Geoscience* **8**, 552-555 (2015).
12. D. G. Pearson, N. Wittig, in *Treatise on Geochemistry (Second Edition),* H. D. Holland, K. K. Turekian, Eds. (Elsevier, Oxford, 2014), pp. 255-292.
13. W. Cao, C.-T. A. Lee, J. S. Lackey, Episodic nature of continental arc activity since 750 Ma: A global compilation. *Earth and Planetary Science Letters* **461**, 85-95 (2017).
14. M. J. Farner, C.-T. A. Lee, Effects of crustal thickness on magmatic differentiation in subduction zone volcanism: A global study. *Earth and Planetary Science Letters* **470**, 96-107 (2017).
15. H. Wang, J. van Hunen, D. G. Pearson, Making Archean cratonic roots by lateral compression: a two-stage thickening and stabilization model. *Tectonophysics* **746**, 562-571 (2018).
16. M. Tang, C.-T. A. Lee, R. L. Rudnick, K. C. Condie, Rapid mantle convection drove massive crustal thickening in the late Archean. *Geochimica et Cosmochimica Acta* **278**, 6-15 (2020).
17. P. G. Silver, M. D. Behn, Intermittent Plate Tectonics? *Science* **319**, 85-88 (2008).
18. K. D. Collerson, B. S. Kamber, Evolution of the Continents and the Atmosphere Inferred from Th-U-Nb Systematics of the Depleted Mantle. *Science* **283**, 1519-1522 (1999).
19. S. W. Parman, Helium isotopic evidence for episodic mantle melting and crustal growth. *Nature* **446**, 900-903 (2007).
20. N. Coltice, B. R. Phillips, H. Bertrand, Y. Ricard, P. Rey, Global warming of the mantle at the origin of flood basalts over supercontinents. *Geology* **35**, 391-394 (2007).

21. A. Lenardic, A supercontinental boost. *Nature Geoscience* **10**, 4-5 (2017).
22. A. Lenardic *et al.*, Continents, supercontinents, mantle thermal mixing, and mantle thermal isolation: Theory, numerical simulations, and laboratory experiments. *Geochemistry, Geophysics, Geosystems* **12**, (2011).
23. G. Zhao, P. A. Cawood, S. A. Wilde, M. Sun, Review of global 2.1–1.8 Ga orogens: implications for a pre-Rodinia supercontinent. *Earth-Science Reviews* **59**, 125-162 (2002).
24. N. M. W. Roberts, The boring billion? – Lid tectonics, continental growth and environmental change associated with the Columbia supercontinent. *Geoscience Frontiers* **4**, 681-691 (2013).
25. P. A. Cawood, R. A. Strachan, S. A. Pisarevsky, D. P. Gladkochub, J. B. Murphy, Linking collisional and accretionary orogens during Rodinia assembly and breakup: Implications for models of supercontinent cycles. *Earth and Planetary Science Letters* **449**, 118-126 (2016).
26. D. C. Bradley, Passive margins through earth history. *Earth-Science Reviews* **91**, 1-26 (2008).
27. P. A. Cawood, Earth Matters: A tempo to our planet's evolution. *Geology* **48**, 525-526 (2020).
28. P. A. Cawood, C. J. Hawkesworth, Earth's middle age. *Geology* **42**, 503-506 (2014).
29. M. Brown, C. L. Kirkland, T. E. Johnson, Evolution of geodynamics since the Archean: Significant change at the dawn of the Phanerozoic. *Geology* **48**, 488-492 (2020).
30. C. Liu, A. H. Knoll, R. M. Hazen, Geochemical and mineralogical evidence that Rodinian assembly was unique. *Nature Communications* **8**, 1950 (2017).
31. T. Rivers, Assembly and preservation of lower, mid, and upper orogenic crust in the Grenville Province—Implications for the evolution of large hot long-duration orogens. *Precambrian Research* **167**, 237-259 (2008).
32. T. Rivers *et al.*, The Grenville Orogen–a post-lithoprobe perspective. *tectonic styles in Canada: The lithoprobe perspective* **49**, 97-236 (2012).
33. C.-T. A. Lee *et al.*, Deep mantle roots and continental emergence: implications for whole-Earth elemental cycling, long-term climate, and the Cambrian explosion. *International Geology Review* **60**, 431-448 (2018).
34. J. Korenaga, N. J. Planavsky, D. A. Evans, Global water cycle and the coevolution of the Earth's interior and surface environment. *Philosophical Transactions of the Royal Society A: Mathematical, Physical and Engineering Sciences* **375**, 20150393 (2017).
35. D. Viviroli, R. Weingartner, B. Messerli, Assessing the hydrological significance of the world's mountains. *Mountain research and Development* **23**, 32-40 (2003).
36. A. L. Zerkle, C. H. House, R. Cox, D. E. Canfield, Metal limitation of cyanobacterial N2 fixation and implications for the Precambrian nitrogen cycle. *Geobiology* **4**, 285-297 (2006).
37. C. Scott *et al.*, Tracing the stepwise oxygenation of the Proterozoic ocean. *Nature* **452**, 456-459 (2008).
38. M. A. Kipp, E. E. Stüeken, Biomass recycling and Earth's early phosphorus cycle. *Science Advances* **3**, eaao4795 (2017).

39. T. A. Laakso, E. A. Sperling, D. T. Johnston, A. H. Knoll, Ediacaran reorganization of the marine phosphorus cycle. *Proceedings of the National Academy of Sciences* **117**, 11961-11967 (2020).
40. N. J. Planavsky, The elements of marine life. *Nature Geoscience* **7**, 855-856 (2014).
41. P. W. Crockford *et al.*, Triple oxygen isotope evidence for limited mid-Proterozoic primary productivity. *Nature* **559**, 613-616 (2018).
42. P. W. Crockford *et al.*, Claypool continued: Extending the isotopic record of sedimentary sulfate. *Chemical Geology* **513**, 200-225 (2019).
43. C. Partin *et al.*, Large-scale fluctuations in Precambrian atmospheric and oceanic oxygen levels from the record of U in shales. *Earth and Planetary Science Letters* **369**, 284-293 (2013).
44. S. Schröder, A. Bekker, N. Beukes, H. Strauss, H. Van Niekerk, Rise in seawater sulphate concentration associated with the Paleoproterozoic positive carbon isotope excursion: evidence from sulphate evaporites in the∼ 2.2–2.1 Gyr shallow-marine Lucknow Formation, South Africa. *Terra Nova* **20**, 108-117 (2008).
45. M. Fakhraee, O. Hancisse, D. E. Canfield, S. A. Crowe, S. Katsev, Proterozoic seawater sulfate scarcity and the evolution of ocean–atmosphere chemistry. *Nature Geoscience* **12**, 375-380 (2019).
46. M. D. Brasier, J. F. Lindsay, A billion years of environmental stability and the emergence of eukaryotes: New data from northern Australia. *Geology* **26**, 555-558 (1998).
47. H. D. Holland, The oxygenation of the atmosphere and oceans. *Philosophical Transactions of the Royal Society B: Biological Sciences* **361**, 903-915 (2006).
48. J. Krissansen-Totton, R. Buick, D. C. Catling, A statistical analysis of the carbon isotope record from the Archean to Phanerozoic and implications for the rise of oxygen. *American Journal of Science* **315**, 275-316 (2015).
49. C. R. Marshall, EXPLAINING THE CAMBRIAN “EXPLOSION” OF ANIMALS. *Annual Review of Earth and Planetary Sciences* **34**, 355-384 (2006).
50. G. A. Shields, A normalised seawater strontium isotope curve: possible implications for Neoproterozoic-Cambrian weathering rates and the further oxygenation of the Earth. *eEarth* **2**, 35-42 (2007).
51. C. P. Bataille, A. Willis, X. Yang, X.-M. Liu, Continental igneous rock composition: A major control of past global chemical weathering. *Science Advances* **3**, e1602183 (2017).
52. T. W. Lyons, C. T. Reinhard, N. J. Planavsky, The rise of oxygen in Earth's early ocean and atmosphere. *Nature* **506**, 307-315 (2014).
53. A. P. Martin, D. J. Condon, A. R. Prave, A. Lepland, A review of temporal constraints for the Palaeoproterozoic large, positive carbonate carbon isotope excursion (the Lomagundi–Jatuli Event). *Earth-Science Reviews* **127**, 242-261 (2013).
54. L. Profeta *et al.*, Quantifying crustal thickness over time in magmatic arcs. *Scientific Reports* **5**, (2015).
55. M. Tang, K. Chen, R. L. Rudnick, Archean upper crust transition from mafic to felsic marks the onset of plate tectonics. *Science* **351**, 372-375 (2016).
56. N. D. Greber *et al.*, Titanium isotopic evidence for felsic crust and plate tectonics 3.5 billion years ago. *Science* **357**, 1271-1274 (2017).

57. C.-T. A. Lee *et al.*, Two-step rise of atmospheric oxygen linked to the growth of continents. *Nature Geosci* **9**, 417-424 (2016).
58. A. D. Burnham, A. J. Berry, Formation of Hadean granites by melting of igneous crust. *Nature Geoscience* **10**, 457-461 (2017).
59. P. W. Hoskin, U. Schaltegger, The composition of zircon and igneous and metamorphic petrogenesis. *Reviews in mineralogy and geochemistry* **53**, 27-62 (2003).
60. C. Herzberg, K. Condie, J. Korenaga, Thermal history of the Earth and its petrological expression. *Earth and Planetary Science Letters* **292**, 79-88 (2010).

Acknowledgments

We thank R. L. Rudnick and C.-T. A. Lee whose comments and suggestions greatly improved the early versions of the manuscript. We also appreciate the insightful discussions with R. McKenzie, Y. Shen, M. Li and P. Liu. We are grateful for the constructive comments from E. J. Chin, P. A. Cawood and an anonymous reviewer. **Funding:** This work was supported by the National Natural Science Foundation of China (42073026, 41888101). M.T. was supported by a Beijing "Double-First Class" initiative grant (7101302526) and a starting fund from Peking University. J.H.H gratefully acknowledges NASA's Astrobiology Institute grant (80NSSC18M0093). **Author contributions:** M.T. initiated the idea and wrote the first manuscript. All authors contributed to data interpretation and manuscript writing. **Competing interests:** The authors declare no competing interests. **Data and materials availability:** All data is available in the manuscript or the supplementary material.